Theory of metallic glasses. I. Electronic structures

W. Y. Ching, Guang-Lin Zhao,* and Yi He
Department of Physics, University of Missouri–Kansas City, Kansas City, Missouri 64110-2499
(Received 6 November 1989)

The electronic structures of three different metallic glasses, a-Ni, a-$Mg_{1-x}Zn_x$, and a-$Cu_{1-x}Zr_x$, are studied by means of the first-principles orthogonalized linear combinations of atomic orbitals (OLCAO) method. Large structural models containing 200 atoms each in a cubic cell with periodic boundary conditions are constructed using the Monte Carlo relaxation method and utilized in the calculation. Results on the density of states (DOS), partial DOS, localization index, effective atomic charges, etc., are presented and discussed. It is emphasized that local short-range order and intermediate-range order, as well as the orbital nature of the constituent atoms, are all important in determining the electronic structures of metallic glasses. Further calculations on metallic glasses with the OLCAO method and other applications of the present results are also discussed.

I. INTRODUCTION

In the past decade, considerable progress has been made in the realistic theoretical calculation of electronic structures of disordered amorphous alloys.[1–8] Electronic structure provides the most basic information that is necessary for the understanding of transport and other properties of disordered alloys at the microscopic level and for the interpretation of many different types of experiments. The unprecedented fast development of computing technology in recent years has facilitated the large-scale computation necessary for the electronic-structure studies of disordered solids. In the study of disordered alloys, it is desirable to distinguish two structurally different disordered alloys: the randomly substituted binary or other multicomponent alloys and the metallic glasses (MG's). The disordered nature of the former comes from the potential fluctuation because of the randomness in the substitution site, which is distributed over a crystalline lattice. In this case, the concept of reciprocal lattice is still valid, and many methods of electronic-structure calculation, which depend on the **k**-space description of the scattering process such as the coherent-potential approximation (CPA) or its derivatives, have been widely used.[9,10] On the other hand, for metallic glasses with one or more atomic species, there is an additional topological disorder associated with the structure of the glass on top of the random distribution of the atomic species. Although the short-range chemical order will be present in most of the MG's, wave vector **k** is no longer a good quantum number and a direct-space approach becomes more appropriate. Atomic models representing the structures of the glasses are the prerequisite for any electronic-structure calculations for MG's. Apart from the less accurate empirical type of calculation, there are two computational approaches corresponding to two different types of boundary conditions of the atomic model. The first is based on the small clusters of atoms with free boundaries and the second is based on the large unit cell with periodic boundary conditions. We prefer the second approach because the periodic model gives a better representation for an infinite solid provided the unit cell is sufficiently large, much larger than the electronic mean free path in the glass. Carefully constructed periodic models are more homogeneous with a correct bulk mass density; and the calculated electronic states will not be contaminated by the surface states.

The direct-space orthogonalized linear combination of atomic orbitals (OLCAO) method has been used to study the electronic structures of noncrystalline solids since mid-1970's. Over the years, the method has been steadily refined and applied to larger and larger periodic model structures for both the insulating glasses[11–13] as well as the metallic glasses[1,3,5] with great success. Since all the interaction integrals, regardless of the interatomic distances and the nature of the local bonding patterns, are evaluated exactly, the method is essentially first-principles in nature. This is particularly important for MG's since both short-range order and intermediate-range order must be accounted for the calculation. This also implies that the resulting electronic wave functions contain all the information about the quantum interference and multiple-scattering effect, which is of paramount importance in the study of transport properties of MG. The use of an atomic-orbital basis also facilitates the interpretation of the results. From a purely computational standpoint, it is much more economic to use an atomic basis than using plane waves. Thus, for a given amount of computer resources, much larger models of MG can be studied by the OLCAO method.

In this paper, we report the results of electronic-structure calculation of three very different glasses using the OLCAO method. They are a-Ni, a-$Mn_{1-x}Zn_x$, and a-$Cu_{1-x}Zr_x$ glasses, each representing a very different class of MG. a-Ni is a single-component, metastable, weakly ferromagnetic transition-metal (TM) glass; a-$Mg_{1-x}Zn_x$ is a free-electron-like glass with many unusual properties; and a-$Cu_{1-x}Zr_x$ is a well-studied glass consisting of the early TM Zr and the late TM Cu. We have used the structural models containing 200 atoms in the cubic cell for the electronic-structure calculation. We have studied previously the electronic structure of the a-

$Cu_{1-x}Zr_x$ glass with only a 90-atom model[3] and *a*-Ni_xP_{1-x} glass with 100-atom models.[5] The present calculation for *a*-$Cu_{1-x}Zr_x$ is therefore a significant extension of the previous study with much larger models and more accurate and rigorously derived potentials. The intercomparison of the electronic structures of these three very different MG's calculated by the same computational method will be highly interesting. In the following paper (referred to as II), we will discuss the calculation of transport and optical properties of the same three MG's based on the results of electronic structures presented in this paper.

The organization of this paper is as follows. We first briefly describe the procedures of model construction in Sec. II. This is followed by a short description of computational procedures in Sec. III. The calculated results for each of the three glasses are presented and discussed in Sec. IV. These results and their implications are further discussed in Sec. V together with some concluding remarks.

II. MODEL CONSTRUCTION

The periodic models were constructed by means of the Monte Carlo relaxation method. For each of the three glasses considered, 200 atoms in a cubic cell of volume L^3 are considered. The cell dimension L is fixed by the mass density of the glass, which is usually extracted from experimental information. A Leonard-Jones type of potential is used to describe the effective interaction between each of the pairs of atoms. The parameters of the potential for *a*-Ni and *a*-$Cu_{1-x}Zr_x$ glass were the same as in the previous work.[3-5] The parameters for the *a*-$Mg_{1-x}Zn_x$ were fixed in a similar fashion by considering the cohesive energies and interatomic distances of crystalline Mg and Zn. A small adjustment in the parameters of the pair potential was made so as to give the first peak position in the calculated radial distribution function of the relaxed model the same as experiment.

The interactions between each pair of atoms up to a distance of $L/2$ were included with periodic boundary condition imposed. Initially, the atoms were randomly distributed in the cell. This corresponds to the case of a high-temperature configuration. The elastic energy of each atom was calculated and the movement of the atom was governed by the standard Monte Carlo algorithm[14] according to the Boltzmann distribution. The fictitious temperature "T" was then successively reduced, accompanied by a graduate reduction in the average elastic energy of the cell, over a period of Monte Carlo steps. After a sufficiently large number of Monte Carlo steps, the total elastic energy stabilized to within 10^{-8} eV per atom and an equilibrium model structure for the glass was obtained.

The quality of these periodic models are very good as judged by the calculated pair correlation functions in comparison with the experimental measurements. A typical case for *a*-$Cu_{60}Zr_{40}$ is shown in Fig. 1 of one of our earlier publications.[15] In spite of the rather modest size of the model, the periodic boundary condition ensures the model representing a truly infinite array of amorphous solid. The cell volume is determined by a number of atoms in the cell so as to give the correct (measured) mass density for the glass. In a cluster type of model which has a free surface, the density cannot be fixed exactly and the simulation process frequently results in inhomogeneous and porous regions in the model. A satisfactory pair-correlation function can be obtained only for sufficiently large models with 1000 atoms or more.

With the periodic models constructed in the above manner, one can study the short-range order of each model in detail and correlate them to the electronic-structure properties. For example, in the one-component glass such as *a*-Ni, the distribution of atoms with a different number of nearest-neighbor (NN) or different average NN distances may be studied. (For a metallic glass, a NN atom is defined as one whose distance of separation is less than the position of the first minimum in the pair-correlation function.) For two- or multicomponent glasses, this can be generalized to include the different cases in which different types of atoms may bind, as was done in Ref. 5 for *a*-$Ni_{1-x}P_x$ glasses.

III. PROCEDURES FOR THE ELECTRONIC STRUCTURE CALCULATION

Since the computational details of the OLCAO method as applied to the amorphous solids have been described amply in the published literature,[3,5] we will only outline the major steps of our calculation, emphasizing the new aspects of the computational detail. Structural models containing 200 atoms in the unit cell as described in II are used for the electronic-structure calculation. Because of the periodic boundary condition, the calculation is identical to that of a band-structure calculation for a simple cubic crystal, but with many atoms in the unit cell. The concept of band dispersion $E(\mathbf{k})$ is no longer valid for amorphous material, and the density of state (DOS) is the essential physical quantity to be obtained. The DOS spectrum is obtained from the energy eigenvalues obtained by diagonalizing the secular equation at the center of the quasi-Brillouin-zone (BZ). As the model becomes larger, this quasi-BZ becomes very small and the energy spectrum at the zone center gives a true representation of the DOS of an infinite amorphous solid. In the cluster type of calculation, the DOS spectrum is also obtained by enumerating the energy eigenvalues from a single diagonalization of the secular equation, except for the fact that the states obtained in this way are contaminated by the surface states because of the free surface of the cluster model.

The calculation starts with the expansion of the solid-state wave function of the amorphous solid in terms of minimal atomic basis sets centered at each atomic site in the model. A minimal basis is one which consists of all the atomic core states plus the complete valence-shell states of the atom, both occupied and unoccupied. For Ni, Cu, and Zn, the valence shell has nine orbitals consisting of 4*s*, 4*p*, and 3*d* atomic states. For Zr, the nine valence orbitals are 5*s*, 5*p*, and 4*d*, and for Mg, only four valence orbitals corresponding to 3*s* and 3*p* states are needed. Such a minimal basis set generally leads to

sufficiently accurate results for the ground-state properties. By means of the core-orthogonalization procedure,[16] the core states are eliminated from the final secular equation so that the final dimension of the matrix equation depends only on the number of atoms in the cell and its valence-shell orbitals. In the present study with 200-atom models, the matrix equations for a-Ni and a-$Cu_{1-x}Zr_x$ have the dimension 1800×1800, while those of a-$Mg_{1-x}Zn_x$ are somewhat smaller.

The potential function for the Mg is constructed from a superposition of atomiclike potentials centered at the atomic sites. In the previous studies[1,3,5] for MG, these potentials were constructed in a partly *ab initio* manner such that when applied to a crystalline band-structure calculation, they yield good results comparable to those obtained by other accurate self-consistent calculations. In the present study, we take a more direct and rigorous approach by first performing a self-consistent OLCAO calculation[17,18] in the simpler pseudocrystalline compounds and using the resulting site-decomposed atomiclike potentials for the amorphous calculation. In the case of binary MG, we use an idealized Cu_3Au structure for the pseudocrystalline calculation. It may be argued that such a procedure is not self-consistent *per se*, since the potentials are derived from the calculation on an idealized structure. We feel that had a truly self-consistent calculation been performed on the 200-atom model, there would be very little difference in the calculated results; present procedure is a best compromise between computation practicality with large model structures and the desired accuracy.

With the basis functions and the potentials well defined, the overlap and the Hamiltonian matrix elements between any pairs of atoms in the unit cell and the adjacent cells are calculated and a supercell lattice sum is performed. This lattice sum converges very rapidly because the unit cell is very large. It is this lattice sum that stems from the quasiperiodicity of the large unit cell that has circumvented the free surface problem encountered in the cluster type of calculations. After the core-orthogonalization process to eliminate the core states, the secular equation is diagonalized and energy eigenvalues and eigenvectors are obtained. From the sampling of the energy eigenvalues, one obtains the DOS. The DOS curves can be resolved into partial components by Mulliken analysis using the wave functions (eigenvectors) obtained for each of the energy eigenstates. The wave function can also be used to calculate the effective charges Q^* and their orbital decompositions. A localization index (LI) for each energy state can also be defined which provides a qualitative measure of the localized or extended nature of the wave function for all the states across the entire energy spectrum. LI ranges from 1 for a 100% localized state to $1/N$ for a 100% delocalized state, where N is the dimension of the secular equation.

It is worthwhile to point out again that a secular equation needs to be solved only at the center of the quasi BZ if the unit cell is large enough. Actually, one can monitor the adequacy of the cell size by comparing the DOS curves obtained from the eigenstates by diagonalization of the secular matrix at the zone center and that at the zone corner. In the present calculation, these two DOS curves are practically the same for a-Ni and a-$Cu_{1-x}Zr_x$ glasses and only slightly different for a-$Mg_{1-x}Zn_x$, indicating that the present cell sizes are sufficiently large for general electronic-structure studies. However, for transport property calculations (to be discussed in paper II), there is another fact related to the size of the cell which may affect the accuracy of the calculation. This is related to the number of states available for dipole transitions in the vicinity of the Fermi level (E_F). This point will be further elaborated in the following paper.[19]

IV. RESULTS AND DISCUSSION

A. a-Ni

The calculated DOS and partial DOS (PDOS) for a-Ni are shown in Fig. 1. Also shown in the same figure for

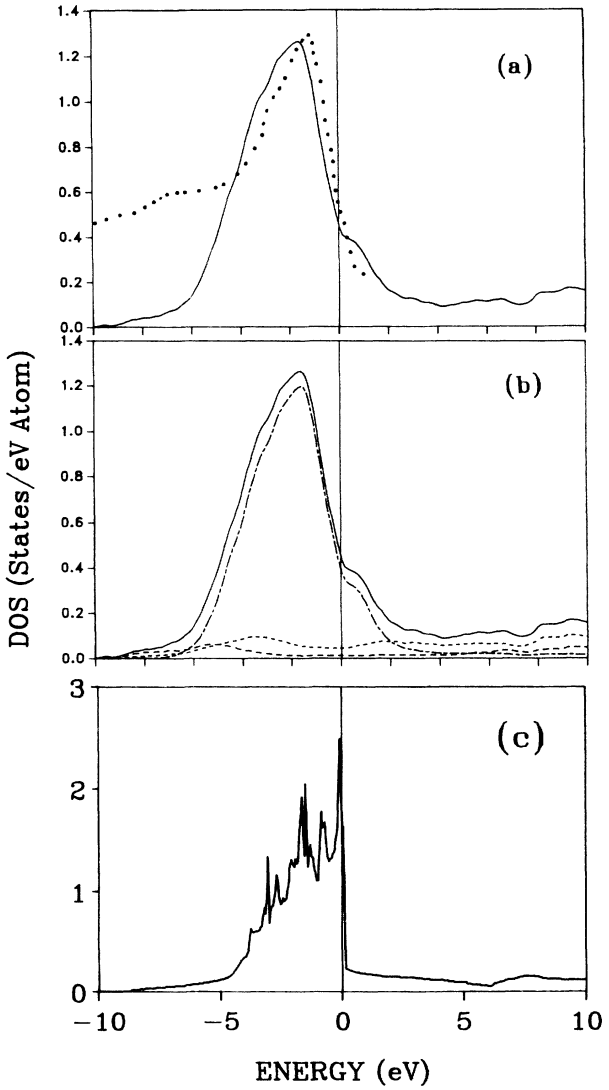

FIG. 1. (a) Total DOS of a-Ni. The dots are the photoemission data for c-Ni from Ref. 19. (b) Partial DOS: dotted line, Ni 4s; dashed line, Ni 4p; dash-dotted line, Ni 4p. The Fermi level is at 0 eV.

comparison is the DOS for fcc crystalline Ni (c-Ni) calculated self-consistently. It is clear that the DOS for a-Ni is dominated by the Ni-3d states and is peaked at about -1.8 eV below E_F. This peak is slightly below the experimental photoemission peak for c-Ni,[20] which is also depicted in Fig. 1. The difference in the peak positions between the theoretical and the experimental curve is not necessarily due to the difference in the long-range order. It could be related to some uncorrected many-body effects. On the whole, we expect the photoemission spectra for c-Ni and a-Ni to be quite similar. The width of the occupied band for a-Ni is about 10 eV. Other than a weak shoulder above the E_F, there is no other prominent structure visible. The E_F cuts at the the steep side of the Ni-3d peak, resulting in what is called a d-band hole. The DOS value at E_F, $N(E_F)$, is 0.47 states/eV. The large number of available states both above and below E_F have rather profound implications in their transport properties.[19]

The LI for states in a-Ni is shown in Fig. 2. As expected, there are highly localized states immediately above and near E_F up to $+2.0$ eV and at about -4 to -10 eV. These are states at the edge of the Ni d band. The majority of states at the center of the d band are relatively delocalized, which is consistent with the formal theory of localization but is opposite to the conventional "wisdom" that all the d states in TM glasses are highly localized. The localized nature of states near E_F is one of the reasons for high resistance in a-Ni or a-$Ni_{1-x}P_x$ MG.[5] The higher conduction band states above 2.0 eV, which consist mainly of 4s and 4p orbitals, are almost completely delocalized.

In Fig. 3, we plot the effective charge Q^* of the 200 Ni atoms. This picture contains much of the microscopic information about the electronic structure of an amorphous metal. Q^* ranges from a high value close to 12 to a low value of less than 2. If we envision the total DOS of Fig. 1 as being formed by a superposition of PDOS of each individual Ni atom with different peak positions, we can see that those Ni atoms with lower peak positions will have all of its ten 3d electrons occupied, while those with higher peak positions will have only a fraction of their 3d electrons occupied. This is because the Fermi level cuts at the d-band edge as discussed above. The precise location of the peak position of the atomic PDOS (and hence its effective charge Q^*) depends on the microscopic short-range order of that atom within the amorphous environment. For atoms with more nearest neighbors and shorter interatomic NN distances, the interatomic interaction will be strong and the peak in the atomic PDOS will be at a lower binding energy and the effective charge will be large. (The NN in an amorphous solid is defined as those atoms whose distances of separation are less than the first minimum in the calculated radial distribution function of the model.) For atoms with fewer nearest neighbors and/or with relatively larger interatomic distances, the peak positions are likely to be higher, resulting in the low Q^* values. It is also obvious from Figs. 2 and 3 that those Ni atoms with low Q^* values are also the ones that give rise to the localized states near the E_F. The above argument is supported by the results shown in Fig. 4 in which we plot the PDOS per Ni atom for different groups of Ni atoms according to the number of NN's. Clearly, the group with least number of NN's has the highest peak positions (lower binding energy) and vice versa. Similar PDOS curves have been obtained in which the Ni atoms were grouped according to their average NN distances.

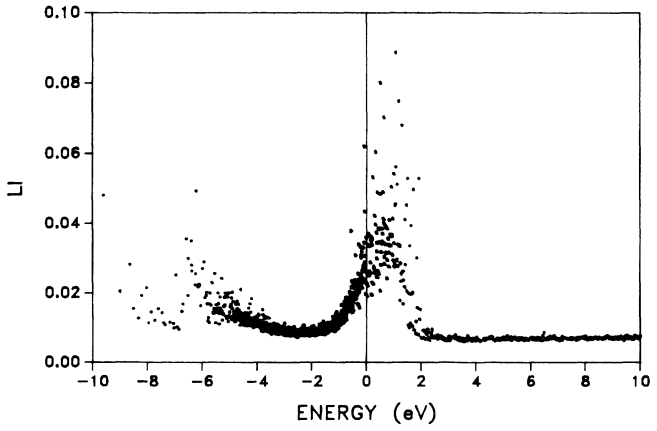

FIG. 2. Localization index (LI) of the states of a-Ni in Fig. 1.

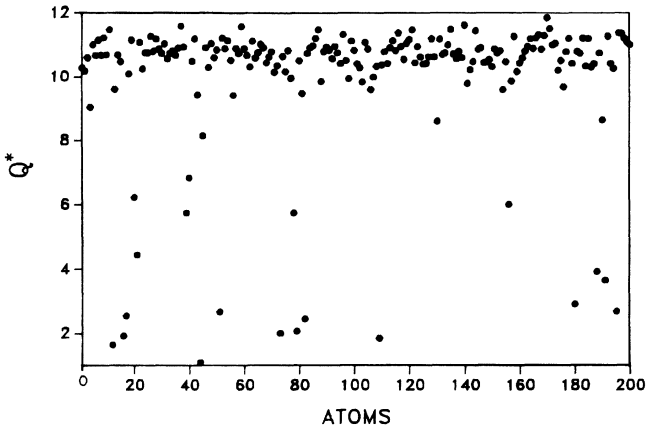

FIG. 3. Effective charge (Q^*) for the 200 Ni atoms in the model.

In the previous study of a-$Ni_{1-x}P_x$ MG,[5] a similar conclusion of a strong dependence of the electronic structure on the local short-range order was obtained. In that study we used a carefully constructed atomiclike potential, which is capable of giving a good bulk band structure for c-Ni, and then implemented an *ad hoc* orbital charge self-consistent procedure[21] to obtain the final electronic structures. The Ni potential used in the present study for a-Ni is directly obtained from the accurate self-consistent band calculation on c-Ni. We have also used the Ni potential used in the a-$Ni_{1-x}P_x$ calculation for the a-Ni study and found a considerable difference in the DOS curves as shown in Fig. 5. The main difference is that the old potential is of shorter range and hence gives a more sharply peaked DOS spectra. This brings us to an

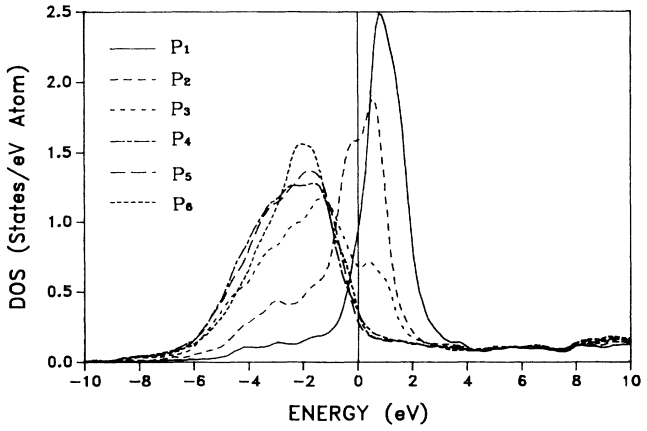

FIG. 4. PDOS per Ni atom of a-Ni according to the number of NN P_i: $P_1=8$, $P_2=9$, $P_3=10$, $P_4=11$, $P_5=12$, and $P_6=13$.

important point: In the study of the electronic structure of MG, not only the local short-range order is important, but also the longer-range interaction that must be reflected. Thus, in parametrized tight-binding-type calculations, only the NN, or at most, the next-NN interactions, are modeled. Therefore it is unlikely to yield accurate results for the electronic structures of most of the glasses.

In Table I we list the numerical values of the orbital-decomposed effective charges and the $N(E_F)$ values for the 200-atom a-Ni calculation

B. a-$Mg_{1-x}Zn_x$

We have calculated the electronic structures of a-$Mg_{1-x}Zn_x$ for $x=0.25$ and 0.30, respectively. The results are very similar and only those of a-$Mn_{75}Zn_{25}$ will be presented. The total DOS averaged over two **k** points for a-$Mg_{75}Zn_{25}$ is shown in Fig. 6. This DOS spectrum is

TABLE I. Calculated results of electronic structure of a-Ni (200-atom model).

Ni 4s	Ni 4p	Ni 3d	Ni total
	effective charges Q^* (electrons)		
0.598	0.098	9.304	10.0
	$N(E_F)$ (states/eV atom)		
0.107	0.014	2.920	3.041

completely different from that of a-Ni, shown in Fig. 1. The DOS is almost featureless as would be expected from a free-electron-like glass. The corelike peak at -8.4 eV corresponds to the Zn 3d states. The free-electron-like states consist of a mixture of Mg 3s, Mg 3p, and Zn 4s orbitals. The DOS value at E_F is very low, only about 0.2 states per eV atom. The extended nature of the free-electron-like states is evident in the LI plot shown in Fig. 7. Apart from the highly localized corelike Zn 3d state, all the states in a-$Mg_{1-x}Zn_x$ are completely delocalized. This is illustrated more clearly in the inset of Fig. 7 for the states near the Fermi level.

The effective charges on the Mg and Zn atoms in a-$Mg_{75}Zn_{25}$ are shown in Fig. 8. The average Q^* for Mg and Zn are 1.79 and 12.63 electrons, respectively, indicating only a slight charge transfer from Mg to Zn. The dispersion in the effective charge distribution in a-$Mg_{75}Zn_{25}$ is much smaller than that of a-Ni, indicating a fundamental difference in the two types of MG. This is because the Zn atom has a closed shell, corelike 3d electrons which are completely localized, and the extended nature of both the s and p orbitals of Zn and Mg are much less sensitive to the local short-range order such as the number of NN's or the average NN distances.

Hafner and Jaswal have also studied the electronic structure of a-$Mg_{70}Zn_{30}$ using the linear muffin-tin orbital (LMTO) method using the 60-atom cell model.[8] Their Zn 3d peak is at a lower binding energy than ours. Also,

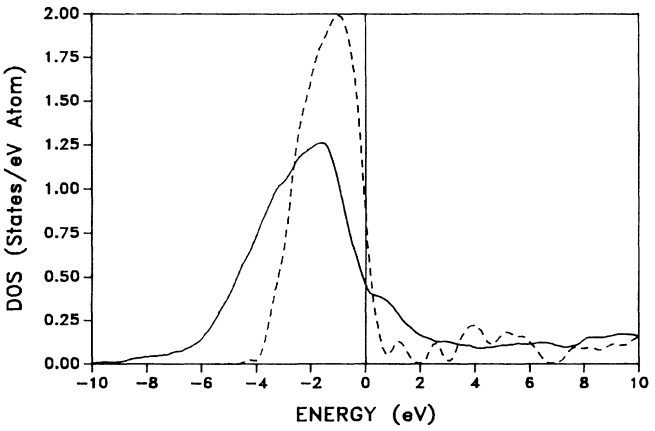

FIG. 5. Comparison of DOS spectrum of a-Ni (solid line) with that calculated with a shorter-range Ni potential (dashed line) (see text).

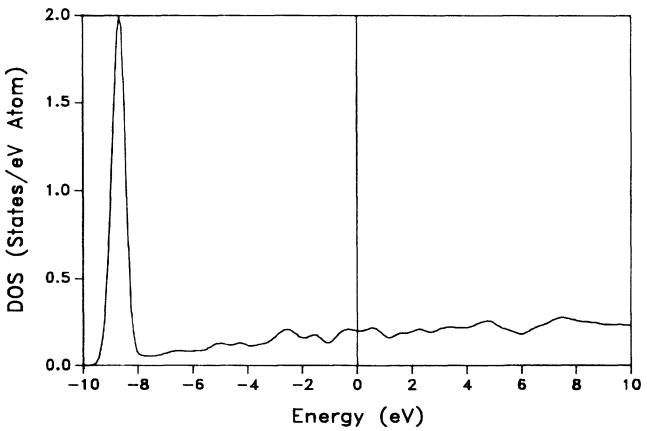

FIG. 6. Total DOS of a-$Mg_{75}Zn_{25}$ averaged over two k points. The peak at -8.6 eV corresponds to the Zn 3d states. The Fermi level is at 0 eV.

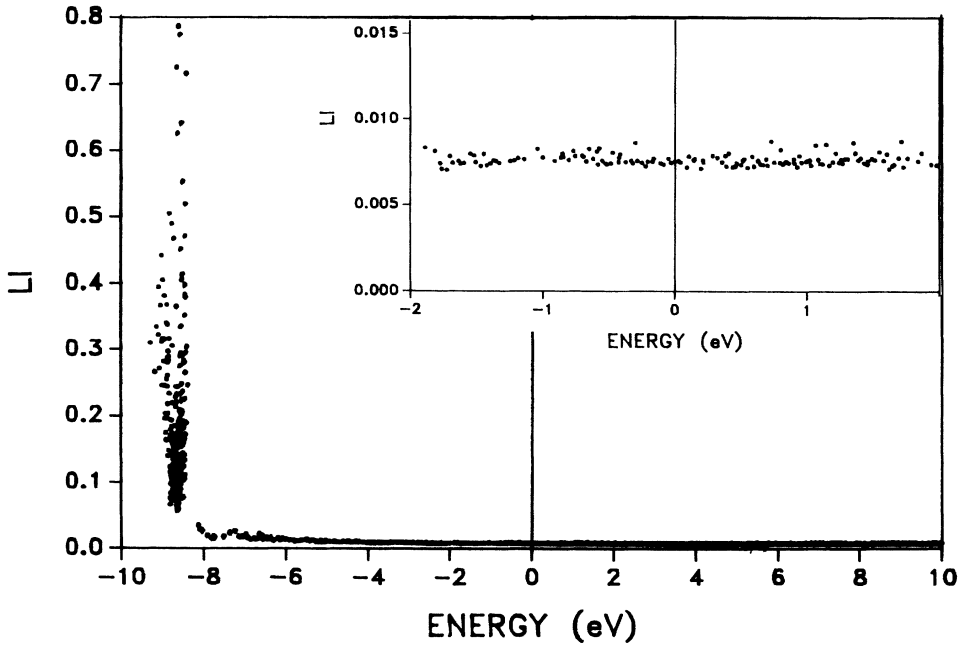

FIG. 7. Localization index of a-$Mg_{75}Zn_{25}$. Inset shows the states near E_F on a finer scale.

they had to use a ten-**k**-point average in order to obtain a reasonably smooth DOS curve. This is, of course, due to the relatively small size of the cell used. However, even in the present study in which we have used a 200-atom cell, there is still a certain degree of fluctuation in the DOS curves calculated at different **k** points. This is shown in Fig. 9, in which we compare the DOS curves obtained at the $\mathbf{k}=(2\pi/a)(0,0,0)$ and $(2\pi/a)(1,1,1)$ points. For TM based glasses, such as a-Ni discussed above and a-$Cu_{1-x}Zr_x$ to be discussed below, models containing only 100 or 90 atoms appear to be able to obtain almost identical DOS curves at different **k** points.[3,5] This contrast is clearly related to the nature of electron mean free path in different MG. In a free-electron-like glass such as a-$Mg_{1-x}Zn_x$, the electron wave functions are very extended and one needs a much larger model to diminish the effect of the quasiperiodicity imposed by the boundary conditions. In TM-based galsses, the electron wave functions are dominated by the d orbitals, which are relatively localized. A 200-atom model is more than sufficient for electronic-structure studies. It is ironic that while a free-electron-like glass is simpler to understand in terms of theoretical models, it is computationally more difficult to obtain accurate results. The same is true for the study of transport properties, which will be further elaborated in paper II.

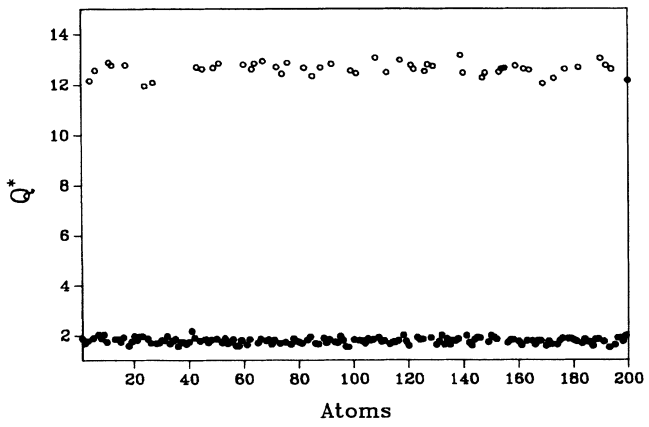

FIG. 8. Effective charges (Q^*) of Mg and Zn atoms in a 200-atom a-$Mg_{75}Zn_{25}$ model. Open circle, Zn atom; solid circle, Mg atom.

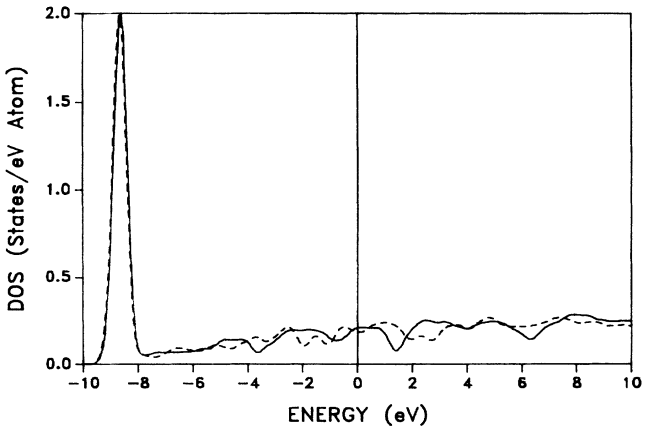

FIG. 9. Comparison of DOS spectra obtained at the zone center (solid curve) and the zone corner (dashed curve) for a-$Mg_{75}Zn_{25}$.

TABLE II. Calculated results of the electronic structure of a-Mg_xZn_{1-x} ($x=0.7,0.75$) (200-atom model).

	Effective charges (electrons)		Charge transfer (electrons)	
	Q^* (Mg)	Q^* (Zn)	ΔQ^* (Mg)	ΔQ^* (Zn)
a-$Mg_{70}Zn_{30}$	1.747	12.591	−0.253	0.591
a-$Mg_{75}Zn_{25}$	1.791	12.627	−0.209	0.627

	$N(E_F)$ (states/eV atom)					
	Mg 3s	Mg 3p	Zn 4s	Zn 4p	Zn 3d	Total
a-$Mg_{70}Zn_{30}$	0.080	0.191	0.035	0.094	0.002	0.402
a-$Mg_{75}Zn_{25}$	0.088	0.196	0.029	0.100	0.002	0.414

In Table II we list the calculated effective charges, the DOS at E_F, and their orbital decompositions for a-$Mg_{75}Zn_{25}$ and a-$Mg_{70}Zn_{30}$ glasses.

C. a-$Cu_{1-x}Zr_x$

a-$Cu_{1-x}Zr_x$ glass is probably the most well studied MG of all. Numerous experimental data on the structural, electronic, transport, and superconducting properties exist[22] and it should serve as a paradigm case for any theory for MG. The electronic structure for a-$Cu_{1-x}Zr_x$ with $x=0.33$, 0.50, and 0.67 has been studied with 90-atom models using the same OLCAO method.[3] The present calculation differs from the previous one in that the 200-atom models are used and atomiclike potentials were derived from fully self-consistent pseudocrystal alloy calculation. Surprisingly, the final results are found to be quite similar to the previous ones. The DOS and the PDOS for a-$Cu_{60}Zr_{40}$ and are shown in Fig. 10. The result for a-$Cu_{50}Zr_{50}$ is not much different and is therefore not presented. The DOS spectrum can be simply interpreted as an overlap of a narrowly peaked Cu 3d band (peaked at −3.80 eV) and a much more broad Zr 4d band. The Fermi level cuts at a local maximum in the Zr 4d band with a $N(E_F)$ value of 0.80 states/eV atom, in agreement with the experimental measurement.[23,24] There is a second broader peak at about 4.0 eV above the E_F. The overlap of the Cu 3d band and the Zr 4d band results in a minimum in the DOS at about −2.30 eV. These features are in very good agreement with the photoemission data,[25,26] which are also reproduced in Fig. 10. Again, the calculated peak position is slightly lower than the experimental peak as expected.

The LI for a-$Cu_{60}Zr_{40}$ is plotted in Fig. 11. It is shown that the states at the edge of the Cu 3d band are relatively

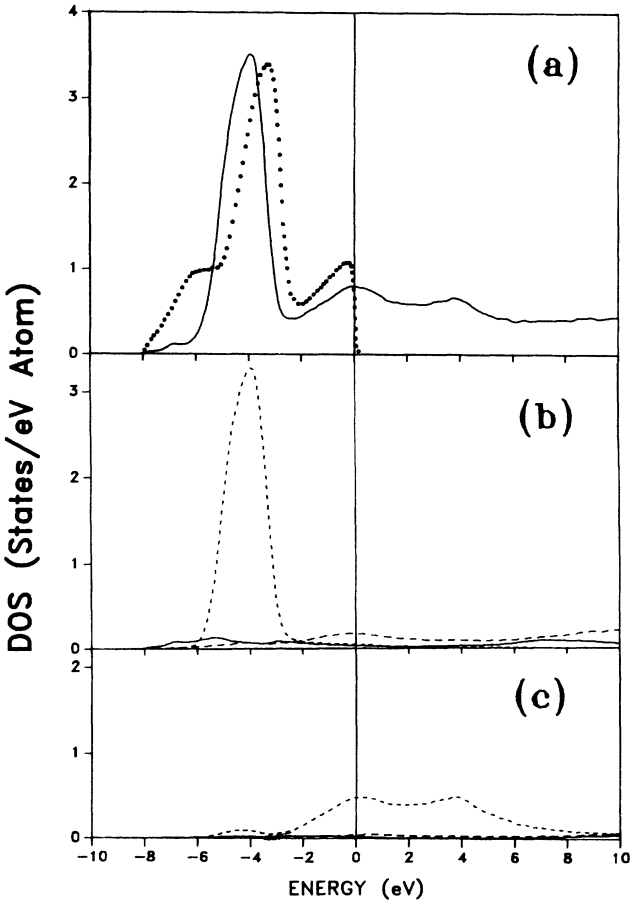

FIG. 10. DOS of a-$Cu_{60}Zr_{40}$: (a) total; dots correspond to the experimental data from Ref. 23. (b) PDOS of Cu: solid line, Cu 4s; dashed line, Cu 4p; dotted line, Cu 3d. (c) PDOS of Zr: solid line, Zr 5s; dashed line, Zr 5p; dotted line, Zr 4d. The Fermi level is at 0 eV.

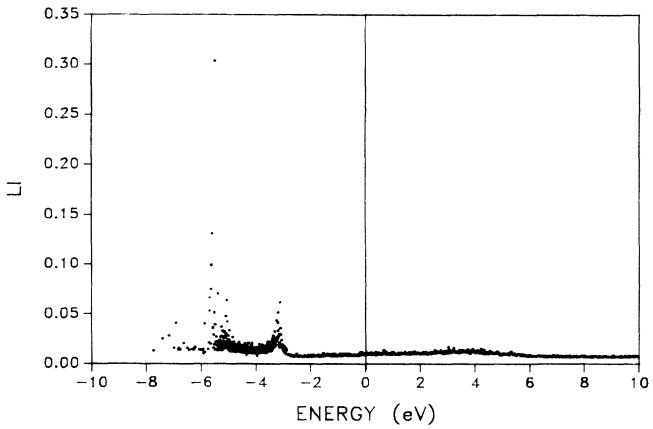

FIG. 11. Localization index of a-$Cu_{60}Zr_{40}$.

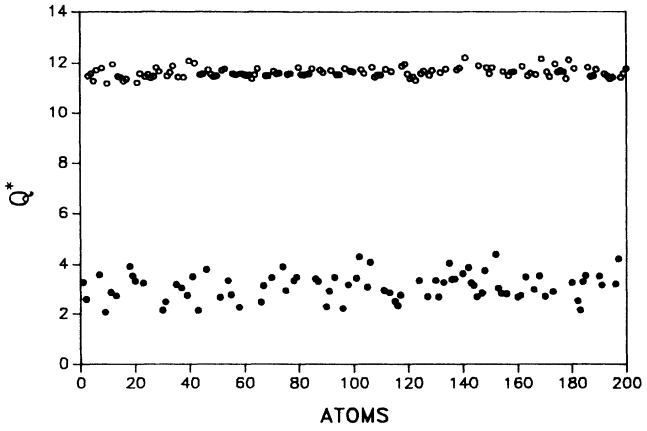

FIG. 12. Effective charge (Q^*) of Cu and Zr atoms in a 200-atom a-$Cu_{60}Zr_{40}$ model. Open circle, Cu atom; solid circle, Zr atom.

localized while those at the edge of the Zr 4d band are not. This is because the Zr 3d band is much wider than the Cu 3d or the Ni 3d band. As a result, the states near E_F in a-$Cu_{60}Zr_{40}$ glass are not highly localized as would be envisioned for a TM glass. On the other hand, they are not as delocalized as those in the free-electron-like MG of a-$Mg_{75}Zn_{25}$ shown in Fig. 7.

The effective charges for Cu and Zr atoms in a-$Cu_{60}Zr_{40}$ are plotted in Fig. 12. The mean values of Q^* are 11.60 electrons or Cu and 3.10 electrons for Zr, indicating a considerable charge transfer from Zr to Cu. Q^* values for Zr actually range from 2.0 to 4.5, while the dispersion for Q^* of Cu is much smaller. This is again due to the larger bandwidth of the Zr band.

In Table III, we list the quantitative values of the orbital-resolved effective charges and the DOS value at E_F for a-$Cu_{60}Zr_{40}$ an a-$Cu_{50}Zr_{50}$. These values are quite similar to the earlier reported values[3] and that deduced from the experiments.[23,24] Although $N(E_F)$ is dominated by the Zr 4d component (68% in a-$Cu_{50}Zr_{50}$ and 62% in a-$Cu_{60}Zr_{40}$), there are substantial admixtures from the free-electron-like s and p orbitals of both Cu and Zr. This makes the formulation of a theory of transport based purely on free-electron scattering extremely difficult. A consistent theory must incorporate the mixed nature of the electron orbitals in a-$Cu_{1-x}Zr_x$ glass.

V. CONCLUSION AND FURTHER DISCUSSION

The simultaneous presentation of the results of electronic structures of three very different MG calculated by the same theoretical method is very revealing. We believe that these are the state-of-the-art results on the electronic-structure calculation for MG. It is shown that the electronic structures of MG are much more complex than previously envisioned. They not only depend on the details of the local short-range order but also the intermediate-range order and on the orbital components of the constituent atoms. A plausible theory for MG must be able to include these fine points. A direct-space large unit-cell approach using the OLCAO method can meet these stringent conditions and provide accurate information on the electronic structures with microscopic details. On the other hand, a theory that uses the radial distribution function as the only input to characterize the disordered nature of a MG will be grossly inadequate. Our calculated result on a-Ni has clearly delineated the important concept that the electronic structure of MG is a superposition of that of individual atoms in the glass, each of which are different depending on their local environment. The measurable properties of MG are most likely to be controlled by those atoms with its electronic states in the vicinity of the Fermi level. Whether these states are localized or extended can only be answered by the realistic large-scale calculation as demonstrated in this paper. Thus, if we were able to introduce a small amount of impurity atoms in a MG such that its local DOS happen to be at E_F, the change in the physical properties of the doped glass will be quite dramatic.

It is now appropriate to discuss the possible further improvement that can be made in the study of electronic structures of MG by the OLCAO method. First, it is always desirable to use even larger models, say with 250–500 atoms per unit cell. This is particularly important for systems with a long electronic mean free path and those with multiatomic species. Such calculations are feasible with the currently available computing facilities. Second, the electronic potentials used in the present calculations can be further improved by performing a

TABLE III. Calculated results of the electronic structure of a-Cu_xZr_{1-x} ($x=0.50, 0.60$) (200-atom model).

	Effective charges (electrons)		Charge transfer (electrons)	
x	Q^*_{Cu}	Q^*_{Zr}	ΔQ^*_{Cu}	ΔQ^*_{Zr}
0.50	11.671	3.329	0.671	−0.671
0.60	11.597	3.104	0.597	−0.896

	$N(E_F)$ (states/eV atom)						
x	Cu 4s	Cu 4p	Cu 3d	Zr 5s	Zr 5p	Zr 4d	Total
0.50	0.022	0.143	0.038	0.025	0.063	0.680	0.893
0.60	0.029	0.169	0.044	0.019	0.046	0.620	0.800

rigorous first-principles self-consistent calculation on smaller models, say with 50–60 atoms per cell, and use the resulting potentials for a bigger model calculation. With further development in the computing technology, this approach can be implemented without any foreseeable difficulty. The way the structure model has been constructed can also be improved. This, however, depends on the availability of more precise, effective interatomic pair potentials. The accurate extraction of pair potentials (with many-body corrections) in metallic systems is still a heavily pursued area of theoretical condensed-matter physics.

The electronic structure is the most basic information needed to understand many different types of experiments in MG. However, to make more direct contact with experiments, it is necessary to calculate directly the physical observable from the energy eigenvalues and electron wave functions obtained in the present study. In the following paper, we present the results of transport and optical properties of the same three MG's studied. We also anticipate to extend our study to MG containing magnetic atoms such as a-$Fe_{1-x}B_x$ in which spin-polarized electronic-structure calculations must be performed. It then becomes possible to study the effect of disorder on the magnetic properties such as localized magnetic moments on each magnetic atom. It is also of much interest to investigate the temperature-dependent properties of MG, starting with electronic-structure calculations on temperature-dependent structural models constructed at different temperatures. These and other results will be the subject of future publications.

ACKNOWLEDGMENTS

This work is supported by the U.S. Department of Energy Grant No. DE-FG02-84ER45170.

*Present address: Department of Physics and Ames Laboratory–U.S. Department of Energy, Iowa State University, Ames, IA 50011-3020.

[1]S. S. Jaswal and W. Y. Ching, Phys. Rev. B **26**, 1064 (1982).
[2]T. Fujiwara, J. Phys. F **12**, 661 (1982).
[3]W. Y. Ching, L. W. Song, and S. S. Jaswal, Phys. Rev. B **30**, 544 (1984); J. Non-Cryst. Solid **61-62**, 1207 (1984).
[4]S. N. Khanna, A. K. Ibrahim, S. W. Mclcuight, and A. Bansil, Solid State Commun. **55**, 223 (1985).
[5]W. Y. Ching, Phys. Rev. B **34**, 2080 (1986).
[6]M. R. Press, S. N. Khanna, and P. Jena, Phys. Rev. B **36**, 5446 (1986).
[7]S. S. Jaswal, Phys. Rev. B **34**, 8937 (1986).
[8]J. Hafner, S. S. Jaswal, M. Tegze, A. Pflugi, J. Krieg, P. Oelhafen, and H. J. Güntherodt, J. Phys. F **18** (1988).
[9]W. H. Butler and G. M. Stocks, Phys. Rev. B **31**, 3260 (1985).
[10]J. C. Swihart, W. H. Butler, G. M. Stocks, D. M. Nicholson, and R. C. Ward, Phys. Rev. Lett. **57**, 1181 (1986).
[11]W. Y. Ching, C. C. Lin, and L. Guttman, Phys. Rev. B **16**, 5488 (1977).
[12]W. Y. Ching, Phys. Rev. Lett. **46**, 607 (1981); Phys. Rev. B **26**, 6632 (1982).
[13]R. A. Murray and W. Y. Ching, J. Non-Cryst. Solid **94**, 144 (1987); Phys. Rev. B **39**, 1320 (1989).
[14]N. Metropolis, A. W. Rosenbluth, M. N. Rosenbluth, A. H. Teller, and E. Teller, J. Chem. Phys. **21**, 1087 (1953).
[15]G.-L. Zhao and W. Y. Ching, Phys. Rev. Lett. **62**, 2511 (1989).
[16]W. Y. Ching and C. C. Lin, Phys. Rev. B **12**, 5536 (1975); **16**, 2989 (1977).
[17]B. N. Harmon, W. Weber, and D. R. Hamann, Phys. Rev. B **25**, 1109 (1982).
[18]W. Y. Ching and B. N. Harmon, Phys. Rev. B **34**, 5305 (1986).
[19]G.-L. Zhao, Yi He, and W. Y. Ching, following paper, Phys. Rev. B **42**, 10 887 (1990).
[20]A. Amamon, D. Aliaga-Guema, P. Panissod, G. Krill, and R. Kuentzler, J. Phys. (Paris) Colloq. **41**, C8-396 (1980).
[21]W. Y. Ching, Solid State Commun. **57**, 385 (1986).
[22]For detailed information see, for example, U. Mizutani, Prog. Mater. Sci. **28**, 2 (1983); M. A. Howson and B. L. Gallagher, Phys. Rep. **170**, 265 (1988).
[23]Z. Altounian and J. O. Strom-Olsen, Phys. Rev. B **27**, 4149 (1983).
[24]K. Samwer and H. v. Löhneysen, Phys. Rev. B **26**, 107 (1982).
[25]P. Oelhafen, E. Hauser, H.-J. Güntherodt, and K. H. Benemann, Phys. Rev. Lett. **43**, 1134 (1979); P. Oelhafen, E. Hauser, and H.-J. Güntherodt, Solid State Commun. **35**, 765 (1980).
[26]P. Oelhafen, in *Glassy Metals II*, edited by H. J. Güntherodt and H. Beck (Springer, New York, 1983), p. 283.